Available online at www.sciencedirect.com
ScienceDirect
Journal of Sound and Vibration 297 (2006) 477–491
JOURNAL OF SOUND AND VIBRATION
www.elsevier.com/locate/jsvi

Dynamic response of a double Euler–Bernoulli beam due to a moving constant load

M. Abu-Hilal

Department of Mechanical and Industrial Engineering, Applied Science Private University, Amman 11931, Jordan

Received 30 March 2005; received in revised form 19 January 2006; accepted 16 March 2006
Available online 27 June 2006

Abstract

In this paper, the dynamic response of a double-beam system traversed by a constant moving load is studied. The system consists of two elastic homogeneous isotropic Euler–Bernoulli beams. The two simply supported prismatic beams are identical, parallel one upon the other and connected continuously by a viscoelastic layer. The dynamic deflections of both beams are given in analytical closed forms. The effects of the moving speed of the load and the damping and the elasticity of the viscoelastic layer on the dynamic responses of the beams are investigated in detail. Also several plots of the deflections of the beams are given and discussed for different values of speed parameter, damping ratio, and stiffness parameter. Furthermore, the force transmitted between the beams is determined and the effects of the system parameters on this force are studied. Plots of the maximum responses of the beams are presented.

1. Introduction

Beams are very important elements in civil, mechanical, and aeronautical engineering. The vibration problem of single beams is very good developed and explored in details in hundreds of contributions. On the other hand, there are only few contributions dealing with the vibrations of double-beam systems, because of the difficulty in solving the governing coupled partial differential equations.

Oniszczuk [1] studied the free vibrations of two parallel simply supported beams continuously joined by a Winkler elastic layer. The eigenfrequencies and mode shapes of vibration of the considered double-beam system have been found using the classical assumed mode summation. Also the presented theoretical analysis is illustrated by a numerical example, in which the effect of physical parameters characterizing the vibrating system on the natural frequencies is investigated. Vu et al. [2] presented an exact method for solving the vibration of a double-beam system subjected to a harmonic excitation. The studied system consists of a main beam with an applied force, and an auxiliary beam, with a distributed spring and dashpot in parallel between the two beams. Oniszczuk [3] analyzed undamped forced transverse vibrations of an elastically connected simply supported double-beam system. The modal expansion method is applied to ascertain dynamic responses of beams due to arbitrarily distributed continuous loads. Several cases of excitation loading are investigated. Shamalta and Matrikine [4] investigated the steady-state dynamic response of an embedded

E-mail address: hilal122@yahoo.com.

0022-460X/$ - see front matter © 2006 Elsevier Ltd. All rights reserved.
doi:10.1016/j.jsv.2006.03.050

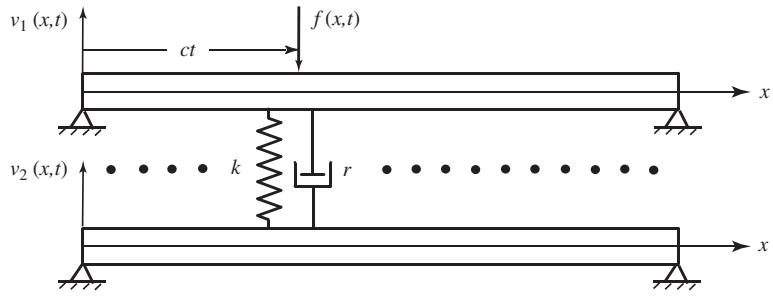

Fig. 1. Double-beam system.

railway track to a moving train. The model for the track consists of a flexible plate performing vertical vibrations, two beams that are connected to the plate by continuous viscoelastic elements and an elastic foundation that supports the plate. Two harmonic loads that move uniformly along the beams describe the train load. The plate, the beams and the elastic foundation are employed to model a concrete slab of an embedded track, the rails and the ground reaction, respectively. Double-beam systems interconnected only at discrete points are investigated in Refs. [5,6]. Also double-string and double-rod systems are studied in Refs. [7–9].

In this paper, the dynamic behavior of a double-beam system traversed by a constant moving load is studied. The system is composed of two elastic prismatic homogeneous isotropic Euler–Bernoulli beams as shown in Fig. 1. The beams are parallel one upon the other arranged and connected continuously by a viscoelastic layer. This layer is modeled as a distributed spring–damper system. The top beam is traversed by a load and is designated as the primary beam. The bottom beam is designated as the secondary beam. In general, the two beams may be different and differently supported. But in order to decouple the governing partial differential equations in a simple way, two restrictions are made: (a) the beams must be identical and (b) the boundary conditions of the same side of the system must be the same [2]. The system studied in this paper consists of two identical simply supported beams. The dynamic deflections of both beams are given in analytical closed forms. The effects of the moving speed of the load and the damping and the elasticity of the viscoelastic layer on the dynamic responses of the beams are investigated in detail. Also several plots of the maximum responses of the beams versus a speed parameter are presented. Furthermore, the force transmitted between the beams is determined and the effects of the system parameters on this force are studied.

2. Mathematical formulation

2.1. Mathematical model and governing equations

The transverse vibration of the double-beam system shown in Fig. 1 is governed by the two coupled partial differential equations.

$$EIv_1'''' + k(v_1 - v_2) + r(\dot{v}_1 - \dot{v}_2) + \mu\ddot{v}_1 = f(x,t), \tag{1}$$

$$EIv_2'''' + k(v_2 - v_1) + r(\dot{v}_2 - \dot{v}_1) + \mu\ddot{v}_2 = 0, \tag{2}$$

where EI is the flexural rigidity of the beam, E is Young's modulus of elasticity, I is the moment of inertia of the cross-sectional area of the beam, μ is the mass per unit length of the beam k is the spring constant of the viscoelastic layer, r is the damping coefficient of the viscoelastic layer, and $v_i(x,t)$ is the transverse deflection of the ith beam at position x and time t. A prime denotes differentiation with respect to position x and a dot denotes differentiation with respect to time t.

The boundary conditions of the studied simply supported beams are

$$v_1(0,t) = v_2(0,t) = 0, \tag{3}$$

$$v_1(L,t) = v_2(L,t) = 0, \tag{4}$$

$$EIv_1''(0,t) = EIv_2''(0,t) = 0, \tag{5}$$

$$EIv_1''(L,t) = EIv_2''(L,t) = 0. \tag{6}$$

In order to decouple Eqs. (1) and (2), let

$$v(x,t) = v_1(x,t) + v_2(x,t). \tag{7}$$

Thus,

$$v_1(x,t) = v(x,t) - v_2(x,t). \tag{8}$$

Adding Eqs. (1) and (2) and considering Eq. (7) leads to

$$EIv'''' + \mu\ddot{v} = f(x,t). \tag{9}$$

Substituting Eq. (8) into Eq. (2) and considering Eq. (7) yields

$$EIv_2'''' + 2kv_2 + 2r\dot{v}_2 + \mu\ddot{v}_2 = f^*(x,t), \tag{10}$$

where the forcing function $f^*(x,t)$ is defined as

$$f^*(x,t) = kv + r\dot{v}. \tag{11}$$

So, two uncoupled partial differential equations (Eqs. (9) and (10)) are obtained. These equations can be easier solved than the coupled Eqs. (1) and (2). First, Eq. (9) is solved, then the obtained solution $v(x,t)$ is substituted into Eq. (11) to obtain the forcing function $f^*(x,t)$ in order to be able to solve Eq. (10). The outcoming solution of this equation represents the deflection $v_2(x,t)$ of the secondary beam. The response $v_1(x,t)$ of the primary beam may be then obtained from Eq. (8). Note that Eq. (10) is identical to the governing partial differential equation of the forced vibration of an Euler–Bernoulli beam on a viscoelastic foundation, whereas Eq. (9) is that of an undamped Euler–Bernoulli beam.

2.2. Solution of Eq. (9)

In modal form, $v(x,t)$ may be given as

$$v(x,t) = \sum_{n=1}^{\infty} X_n(x) y_n(t), \tag{12}$$

where $y_n(t)$ is the generalized deflection of the nth mode and $X_n(x)$ is the nth eigenfunction of a simply supported beam defined as

$$X_n(x) = \sin \kappa_n x \tag{13}$$

with

$$\kappa_n = \frac{n\pi}{L}. \tag{14}$$

Substituting Eq. (12) into Eq. (9) and then multiplying by $X_f(x)$, and integrating with respect to x between 0 and L leads to

$$\ddot{y}_n + \omega_n^2 y_n = Q_n(t) \tag{15}$$

with the circular frequency of the nth mode

$$\omega_n = \sqrt{\frac{k_n}{m_n}} = \kappa_n^2 \sqrt{\frac{EI}{\mu}}, \tag{16}$$

where

$$k_n = \int_0^L EIX_n'''' X_n \,\mathrm{d}x \tag{17}$$

is the generalized stiffness of the nth mode and

$$m_n = \int_0^L \mu X_n^2(x)\,\mathrm{d}x = \frac{\mu L}{2} \tag{18}$$

is the generalized mass of the nth mode.

A constant force P_0 traversing the beam from the left-hand side with constant speed so that the load $f(x,t)$ is defined as

$$f(x,t) = P_0\delta(x - ct), \tag{19}$$

where $\delta(.)$ denotes the Dirac delta function. The generalized force associated with the nth mode is then given as

$$Q_n(t) = \frac{1}{m_n}\int_0^L X_n(x) f(x,t)\,\mathrm{d}x = \frac{2P_0}{\mu L}\sin(\kappa_n ct). \tag{20}$$

Assuming that the beams are originally at rest, i.e.

$$v_1(x,0) = v_2(x,0) = \dot{v}_1(x,0) = \dot{v}_2(x,0) = 0 \tag{21}$$

the solution of Eq. (15) is then written as

$$y_n(t) = \int_0^t h_n(t-\tau) Q_n(\tau)\,\mathrm{d}\tau, \tag{22}$$

where $h_n(t)$ is the impulse response function defined as

$$h_n(t) = \begin{cases} \frac{\sin\omega_n t}{\omega_n} & t \geqslant 0, \\ 0 & t < 0. \end{cases} \tag{23}$$

Substituting Eqs. (20) and (23) into Eq. (22) yields

$$y_n(t) = \frac{2P_0}{\mu L \omega_n}\int_0^t \sin\omega_n(t-\tau)\sin\kappa_n c\tau\,\mathrm{d}\tau. \tag{24}$$

Carrying out the integration and substituting the obtained result into Eq. (12) gives the solution of Eq. (9) in the form

$$v(x,t) = \frac{2P_0}{\mu L}\sum_{n=1}^{\infty}\frac{\sin\kappa_n x}{(\kappa_n c)^2 - \omega_n^2}\left[\frac{\kappa_n c}{\omega_n}\sin\omega_n t - \sin\kappa_n ct\right]. \tag{25}$$

Note that $v(x,t)$ is independent on the layer damping.

2.3. Deflection of the secondary beam

Substituting Eq. (25) and its time derivative into Eq. (11) yields

$$f^*(x,t) = \frac{2P_0}{\mu L}\sum_{n=1}^{\infty}\sin\kappa_n x q_n(t), \tag{26}$$

where

$$q_n(t) = \frac{1}{(\kappa_n c)^2 - \omega_n^2}\left\{k\left[\frac{\kappa_n c}{\omega_n}\sin\,\omega_n t - \sin\,\kappa_n ct\right] + r\kappa_n c[\cos\,\omega_n t - \cos\,\kappa_n ct]\right\}. \tag{27}$$

Substituting Eq. (26) into Eq. (10) leads to

$$EIv_2'''' + 2kv_2 + 2r\dot{v}_2 + \mu\ddot{v}_2 = \frac{2P_0}{\mu L}\sum_{n=1}^{\infty}\sin\kappa_n x q_n(t). \tag{28}$$

Solving this equation yields the deflection $v_2(x,t)$ of the secondary beam. In modal form, $v_2(x,t)$ may be given as

$$v_2(x,t) = \sum_{n=1}^{\infty} X_{2n}(x) y_{2n}(t), \tag{29}$$

where $y_{2n}(t)$ is the generalized deflection of the nth mode and $X_{2n}(x)$ is the nth normal mode defined as

$$X_{2n}(x) = \sin\lambda_n x \tag{30}$$

with

$$\lambda_n = \frac{n\pi}{L}. \tag{31}$$

Substituting Eq. (29) into Eq. (28) and then multiplying by $X_j(x)$, and integrating with respect to x between 0 and L leads to

$$\ddot{y}_{2n}(t) + 2\Omega_n\zeta_n\dot{y}_{2n}(t) + \Omega_n^2 y_{2n}(t) = Q_n^*(t), \tag{32}$$

where

$$\Omega_n = \sqrt{\frac{EI\lambda_n^4 + 2k}{\mu}} \tag{33}$$

is the circular frequency of the nth mode and

$$\zeta_n = \frac{r}{\mu\Omega_n} \tag{34}$$

is the damping ratio of the nth mode. The generalized force associated with the nth mode Q_n^* is given as

$$Q_n^*(t) = \frac{1}{m_n}\int_0^L X_{2j}(x)\frac{2P_0}{\mu L}\sum_{n=1}^{\infty}\sin(\kappa_n x)q_n(t)\,\mathrm{d}x, \tag{35}$$

where m_n is the generalized mass as defined in Eq. (18). Carrying out the integration and using the orthogonality relationship

$$\int_0^L X_n X_k\,\mathrm{d}x = 0, \quad n \neq k \tag{36}$$

leads to

$$Q_n^*(t) = \frac{2P_0}{\mu^2 L}q_n(t), \tag{37}$$

where $q_n(t)$ is defined in Eq. (27). Assuming the beams are originally at rest, the solution of Eq. (32) is then written as

$$y_{2n}(t) = \int_0^t h_n^*(t-\tau)Q_n^*(\tau)\,\mathrm{d}\tau, \tag{38}$$

where $h_n^*(t)$ is the impulse response function defined for $0 \leq \zeta_n < 1$ as

$$h_n^*(t) = \begin{cases} \frac{1}{\Omega_{dn}}\mathrm{e}^{-\zeta_n\Omega_n t}\sin\Omega_{dn}t, & t \geq 0, \\ 0, & t < 0 \end{cases} \tag{39}$$

in which

$$\Omega_{dn} = \Omega_n \sqrt{1-\zeta_n^2} \tag{40}$$

is the damped circular frequency of the nth mode. Substituting Eqs. (37) and (39) into Eq. (38) yields

$$y_{2n}(t) = \frac{2P_0 e^{-\zeta_n \Omega_n t}}{\mu^2 L \Omega_{dn}} \int_0^t e^{\zeta_n \Omega_n \tau} \sin \Omega_{dn}(t-\tau) q_n(\tau)\, d\tau. \tag{41}$$

Carrying out the integration gives

$$\begin{aligned} y_{2n}(t) = {} & a_{1n}\frac{\kappa_n c}{\omega_n}[(a_{3n}a_{6n} - a_{2n}a_{4n})\cos\omega_n t + (a_{2n}a_{5n} - a_{3n}a_{7n})\sin\omega_n t] \\ & + a_{1n}[(a_{8n}a_{12n} - a_{10n}a_{13n})\cos\kappa_n c t + (a_{11n}a_{13n} - a_{9n}a_{12n})\sin\kappa_n c t] \\ & + a_{1n}\left[\frac{\kappa_n c}{\omega_n}(a_{2n}a_{4n} - a_{3n}a_{6n}) + (a_{10n}a_{13n} - a_{8n}a_{12n})\right] e^{-\zeta_n \Omega_n t}\cos\Omega_{dn} t \\ & - a_{1n}\left[\frac{\kappa_n c}{\omega_n}(a_{2n}a_{5n} + a_{3n}a_{7n}) - (a_{11n}a_{13n} + a_{9n}a_{12n})\right] e^{-\zeta_n \Omega_n t}\sin\Omega_{dn} t, \end{aligned} \tag{42}$$

where

$$a_{1n} = \frac{P_0}{\mu^2 L \Omega_{dn}} \frac{1}{(\kappa_n c)^2 - \omega_n^2},$$

$$a_{3n} = \frac{1}{(\zeta_n \Omega_n)^2 + (\Omega_{dn} + \omega_n)^2},$$

$$a_{3n} = \frac{1}{(\zeta_n \Omega_n)^2 + (\Omega_{dn} + \omega_n)^2},$$

$$a_{4n} = \zeta_n \Omega_n k - (\Omega_{dn} - \omega_n) r \omega_n,$$

$$a_{5n} = \zeta_n \Omega_n r \omega_n + (\Omega_{dn} - \omega_n) k,$$

$$a_{6n} = \zeta_n \Omega_n k + (\Omega_{dn} + \omega_n) r \omega_n,$$

$$a_{7n} = \zeta_n \Omega_n r \omega_n - (\Omega_{dn} + \omega_n) k,$$

$$a_{8n} = \zeta_n \Omega_n k - (\Omega_{dn} - \kappa_n c) r \kappa_n c,$$

$$a_{9n} = \zeta_n \Omega_n r \kappa_n c + (\Omega_{dn} - \kappa_n c) k,$$

$$a_{10n} = \zeta_n \Omega_n k + (\Omega_{dn} + \kappa_n c) r \kappa_n c,$$

$$a_{11n} = \zeta_n \Omega_n r \kappa_n c - (\Omega_{dn} + \kappa_n c) k,$$

$$a_{12n} = \frac{1}{(\zeta_n \Omega_n)^2 + (\Omega_{dn} - \kappa_n c)^2},$$

$$a_{13n} = \frac{1}{(\zeta_n \Omega_n)^2 + (\Omega_{dn} + \kappa_n c)^2}. \tag{43a–m}$$

After substituting $y_{2n}(t)$ as given in Eq. (42) into Eq. (29), the deflection of the secondary beam is known. The deflection of the primary beam is obtained from Eq. (8), where $v(x,t)$ and $v_2(x,t)$ are given in Eqs. (25) and (29), respectively.

2.4. The Force transmitted between the beams

The force transmitted between the two beams is defined as

$$F_T = k(v_1 - v_2) + r(\dot{v}_1 - \dot{v}_2). \tag{44}$$

Using Eqs. (8), (25), (29), and (42) yields for the force transmitted:

$$\begin{aligned} F_T = \frac{P_0}{\mu L}\sum_{n=1}^{\infty}\frac{\sin\kappa_n x}{\Omega_{dn}}\big[[a_{10n}a_{13n} - a_{8n}a_{12n}]\cos\kappa_n ct + [a_{9n}a_{12n} - a_{11n}a_{13n}]\sin\kappa_n ct \\ - [a_{9n}a_{12n} + a_{11n}a_{13n}]\mathrm{e}^{-\zeta_n\Omega_n t}\sin\Omega_{dn}t \\ +[a_{13n}a_{14n} + a_{12n}a_{15n}]\mathrm{e}^{-\zeta_n\Omega_n t}\cos\Omega_{dn}t\big], \end{aligned} \tag{45}$$

where a_{8n} to a_{13n} are defined in Eq. (43) and

$$\begin{aligned} a_{14n} &= -k\zeta_n\Omega_n + r(\Omega_n^2 + \Omega_{dn}\kappa_n c), \\ a_{15n} &= k\zeta_n\Omega_n - r(\Omega_n^2 - \Omega_{dn}\kappa_n c). \end{aligned} \tag{46a,b}$$

3. Results and discussion

In order to illustrate the obtained analytical solutions, the dimensionless deflections

$$\bar{v}_i = \frac{v(L/2,s)}{v_0}, \quad i = 1,2 \tag{47}$$

versus the dimensionless time s are given for both beams where only the first term of summation is considered. The symbol v_0 designates the static deflection at mid-span of a simply supported beam loaded with a static force P_0 at point $x = L/2$ and is defined as

$$v_0 = \frac{P_0 L^3}{48EI}. \tag{48}$$

The dimensionless time is defined as

$$s = \frac{ct}{L}. \tag{49}$$

Thus when $s = 0$ the force is at the left-hand side of the beam and when $s = 1$ the force is at the right-hand side of the beam.

The constant force P_0 enters the upper beam at rest from the left-hand side at position $x = 0$ and moves to the right with constant speed c. The effect of speed is represented by the dimensionless speed parameter α, where

$$\alpha = \frac{c}{c_{cr}}, \tag{50}$$

with the critical speed c_{cr} defined as [10]

$$c_{\mathrm{cr}} = \frac{\omega_1 L}{\pi}, \tag{51}$$

where

$$\omega_1 = \left(\frac{\pi}{L}\right)^2\sqrt{\frac{EI}{\mu}}. \tag{52}$$

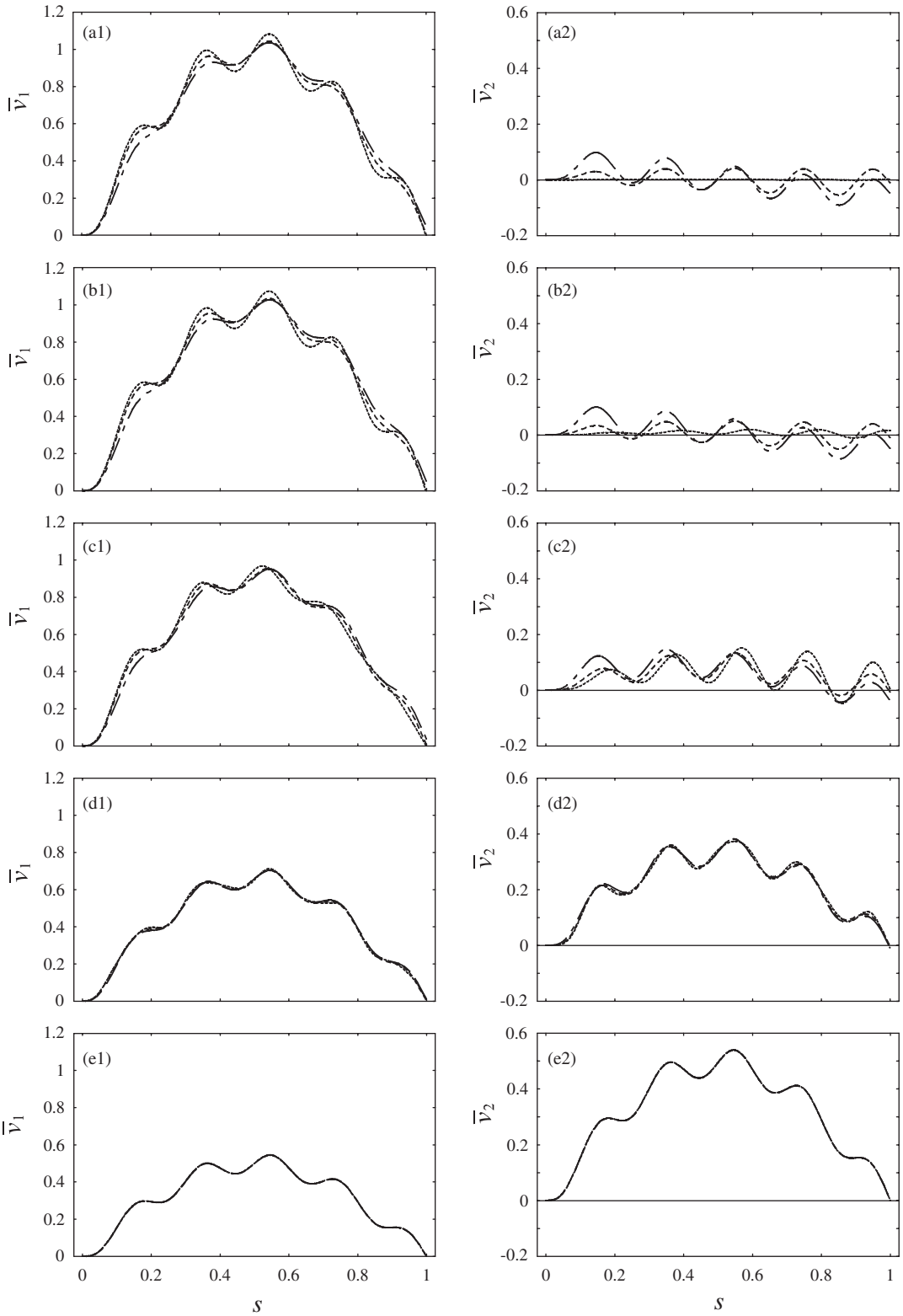

Fig. 2. Dimensionless dynamic deflection versus the normalized time for primary beam ($\bar{v}_1$) and secondary beam ($\bar{v}_2$) for a speed factor $\alpha = 0.1$, (a_i) $\beta = 0.1$, (b_i) $\beta = 1$, (c_i) $\beta = 10$, (d_i) $\beta = 100$, (e_i) $\beta = 10\,000$, $i = 1, 2$, (———) $\zeta = 0$, (- - - -) $\zeta = 0.1$, (— · — · —) $\zeta = 0.5$.

The effect of the layer stiffness k is represented by the dimensionless parameter

$$\beta = \frac{kL^4}{EI}. \tag{53}$$

Fig. 2 shows the dimensionless deflections for the primary ($\bar{v}_1$) and secondary ($\bar{v}_2$) beams for a speed factor $\alpha = 0.1$ and different values of damping ratio ζ and stiffness parameter β. From Figs. $2a_1$–e_1 it is observable that dependent on the dimensionless time s, the deflection $\bar{v}_1$ may be decreased or increased by increasing the values of the damping ratio ζ. Also the absolute maximum value of $\bar{v}_1$ is reached short after the load crosses the mid-span of the beam. Furthermore, the figures show that increasing the values of the stiffness parameter β leads to a decrease in the dimensionless deflection $\bar{v}_1$, where values of β smaller than 0.1 or higher than 10^4 have irrelevant influence on the dimensionless deflection $\bar{v}_1$. In the absence of damping, very small values of β means that the two beams are decoupled (weak elastic coupling). However, increasing the values of β leads to increasing the coupling between the two beams where very high values of β leads to rigid-coupling of the beams.

From Figs. $2a_1$–e_1 it is noticeable that the values of $\bar{v}_1$ by rigid-coupling ($2e_1$) are reduced down to 50% of the values of $\bar{v}_1$ for the uncoupled system ($2a_1$). Furthermore, the damping effect becomes smaller with increasing the values of the stiffness parameter β.

Figs. $2a_2$–e_2 show the dimensionless dynamic deflection $\bar{v}_2$ for the secondary beam. From these figures it is observed that increasing the values of stiffness parameter β increases the deflection $\bar{v}_2$. Very high values of β (Fig. $2e_2$) cause rigid-coupling between the two beams so that they vibrate together as a unit. Consequently, the normalized deflection $\bar{v}_2$ equals $\bar{v}_1$ in this case.

For very small values of stiffness parameter β (Fig. 2-a_2), which means weak elastic coupling, the dimensionless deflection $\bar{v}_2$ is increased by increasing the values of the damping ratio ζ. That is because increasing the values of ζ increases the coupling between the two beams so that higher mechanical energy will be transmitted from the primary to the secondary beam. Consequently, the excitation forces acting on the secondary beam are increased.

From Figs. $2a_2$–e_2 it is observed that the effect of damping on the normalized deflection $\bar{v}_2$ becomes smaller by increasing the values of the stiffness parameter β.

Fig. 3 shows dimensionless deflections for the primary ($\bar{v}_1$) and secondary ($\bar{v}_2$) beams for a speed factor $\alpha = 0.25$ and different values of damping ratio ζ and stiffness parameter β. The figure shows that, in general, the system behaves as in the case for a speed factor $\alpha = 0.1$. But from Fig. 3 it is observable that the absolute maximum values of $\bar{v}_1$ and $\bar{v}_2$ occur at the time at which the load traversed ca. 40% of the beam's length. However the absolute maximum value of $\bar{v}_2$ occurs a little earlier for relative small values of β. Figs. $3a_1$–c_1 show that the absolute maximum value of $\bar{v}_1$ occurs at a later time by increasing the damping ratio ζ. From the figures it is furthermore observable that increasing the damping ratio may, depending on the dimensionless time s, increases or decreases the values of $\bar{v}_1$. To be specific, from Fig. $3a_1$ it is evident to see that for values of s between 0 and 0.5, increasing the values of ζ decreases the values of $\bar{v}_1$. However, for values of s between ca. 0.5 and ca. 0.8, increasing the values of ζ leads to an increase in the values of $\bar{v}_1$.

Fig. $3a_2$–c_2 show that the absolute maximum value of $\bar{v}_2$ occurs at an earlier time by increasing the damping ratio ζ.

Fig. 4 shows the dimensionless deflections for the primary ($\bar{v}_1$) and secondary ($\bar{v}_2$) beams for a speed factor $\alpha = 0.5$ and different values of damping ratio ζ and stiffness parameter β. The figure shows that increasing the values of the stiffness parameter β decreases the deflection $\bar{v}_1$. In the case of rigid-coupling (Fig. $4e_1$), the value of $\bar{v}_1$ is reduced down to 50% of $\bar{v}_1$ for the uncoupled beam. Also as previously stated, the values of $\bar{v}_1$ may be decreased or increased by increasing the values of damping ratio ζ. The absolute maximum value of $\bar{v}_1$ is reached in the time interval in which the load travels between 0.5 and 0.7 of the beams span. This value is delayed by increasing the value of the damping ratio ζ.

Fig. $4a_2$–e_2 show that increasing the value of the stiffness parameter β increases the dimensionless deflection $\bar{v}_2$. In the case of rigid-coupling, $\bar{v}_2$ equals $\bar{v}_1$. Furthermore, it is observed that the absolute maximum value of $\bar{v}_2$ is reached after the load traversed 60% of the beam's length, but before the load left the beam. This value occurs earlier by increasing the value of the damping ratio.

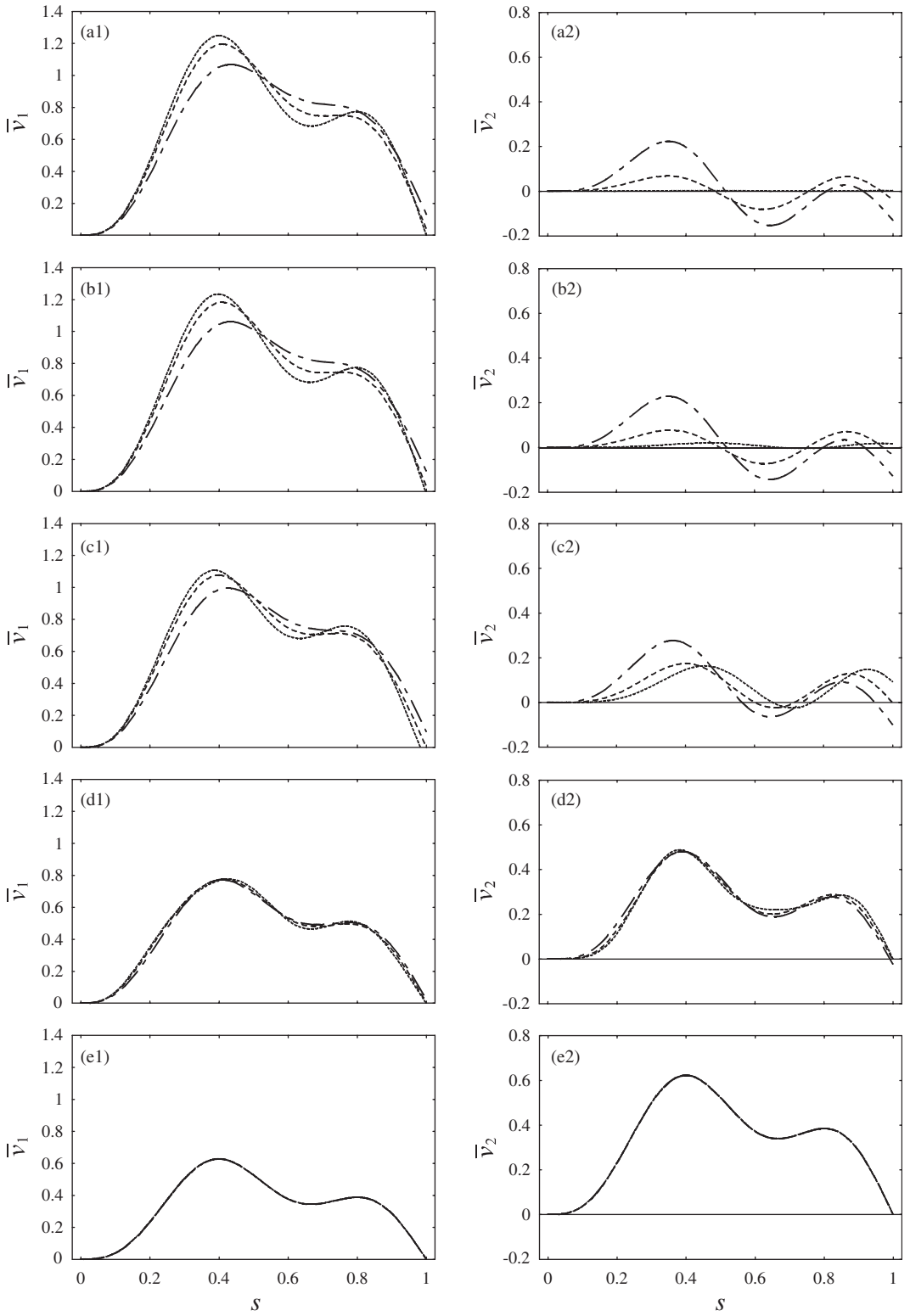

Fig. 3. Dimensionless dynamic deflection versus the normalized time for primary beam ($\bar{v}_1$) and secondary beam ($\bar{v}_2$) for a speed factor $\alpha = 0.25$, (a_i) $\beta = 0.1$, (b_i) $\beta = 1$, (c_i) $\beta = 10$, (d_i) $\beta = 100$, (e_i) $\beta = 10\,000$, $i = 1, 2$, (———) $\zeta = 0$, (- - - -) $\zeta = 0.1$, (— · — · —) $\zeta = 0.5$.

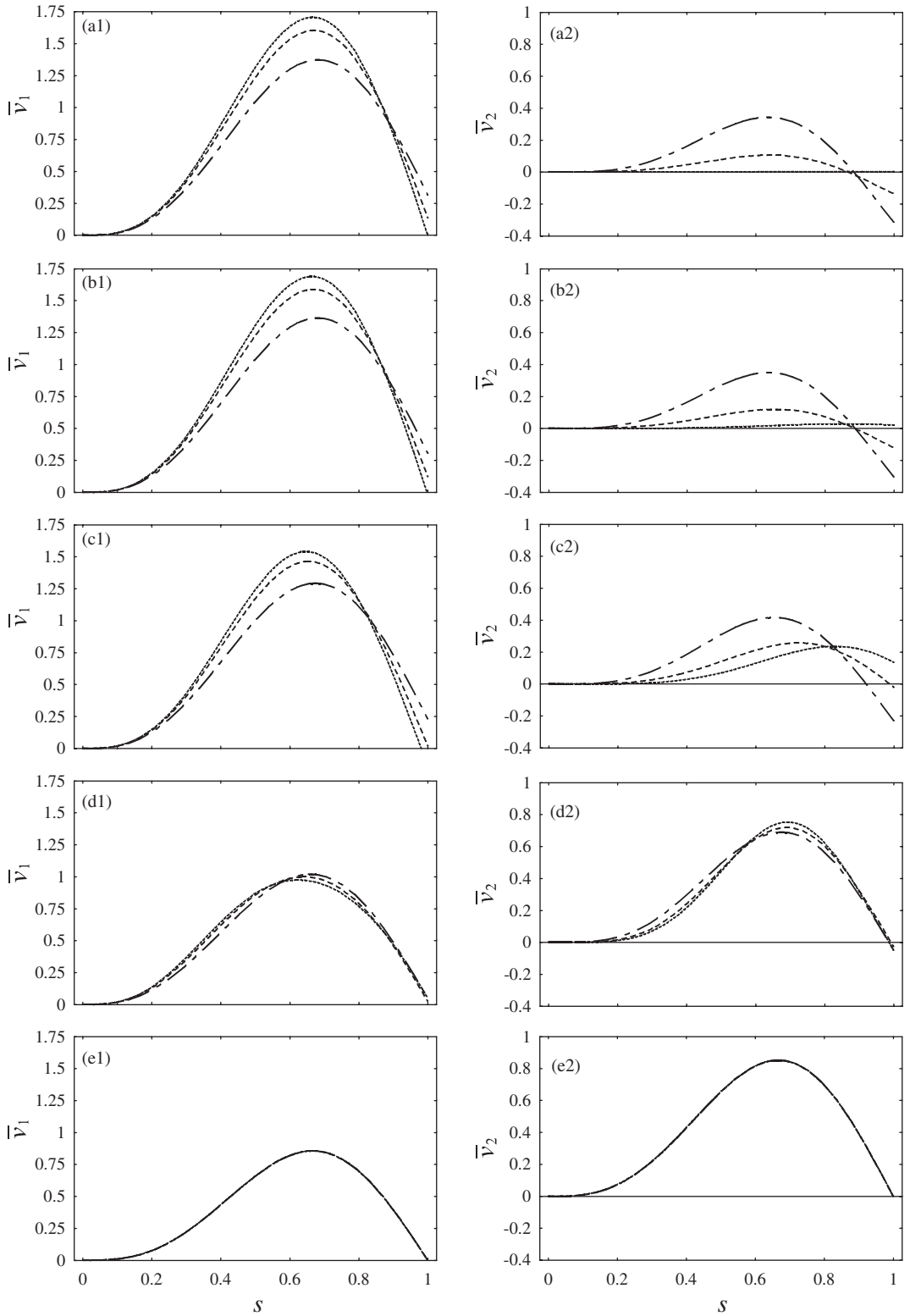

Fig. 4. Dimensionless dynamic deflection versus the normalized time for primary beam ($\bar{v}_1$) and secondary beam ($\bar{v}_2$) for a speed factor $\alpha = 0.5$, (a_i) $\beta = 0.1$, (b_i) $\beta = 1$, (c_i) $\beta = 10$, (d_i) $\beta = 100$, (e_i) $\beta = 10\,000$, $i = 1, 2$, (———) $\zeta = 0$, (- - - -) $\zeta = 0.1$, (— · — · —) $\zeta = 0.5$.

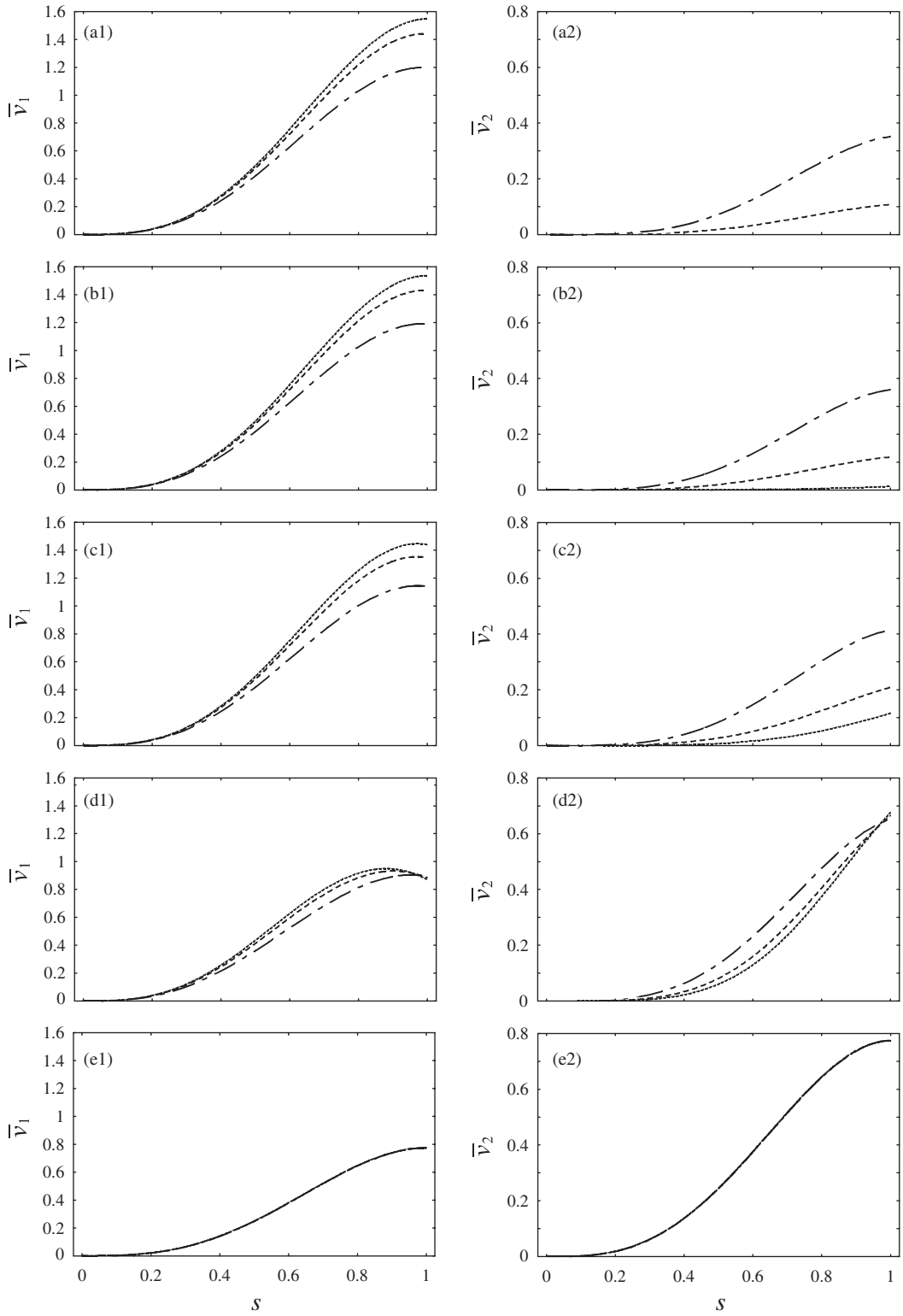

Fig. 5. Dimensionless dynamic deflection versus the normalized time for primary beam ($\bar{v}_1$) and secondary beam ($\bar{v}_2$) for a speed factor $\alpha = 1$, (a_i) $\beta = 0.1$, (b_i) $\beta = 1$, (c_i) $\beta = 10$, (d_i) $\beta = 100$, (e_i) $\beta = 10\,000$, $i = 1, 2$, (———) $\zeta = 0$, (- - - -) $\zeta = 0.1$, (— · — · —) $\zeta = 0.5$.

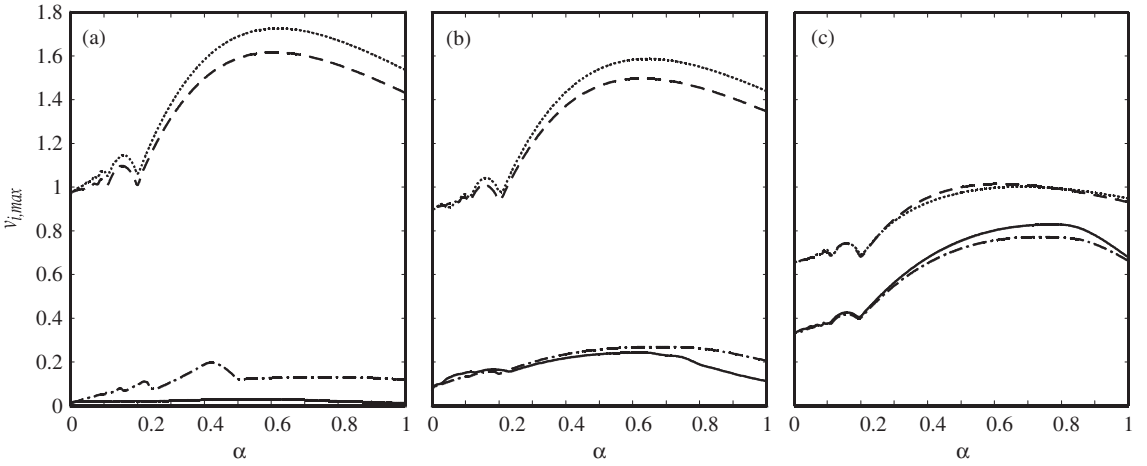

Fig. 6. Maximum deflections $\bar{v}_{1,\max}$ and $\bar{v}_{2,\max}$ versus the speed parameter α for different values of stiffness parameter β and damping ratio ζ calculated at $x = L/2$: (… …)$\bar{v}_{1,\max}$, $\zeta = 0$, (- - - -) $\bar{v}_{1,\max}$,$\zeta = 0.1$, (———) $\bar{v}_{2,\max}$, $\zeta = 0$, (— · — · —) $\bar{v}_{2,\max}$, $\zeta = 0.1$, (a) $\beta = 1$, (b) $\beta = 10$, (c) $\beta = 100$.

Fig. 5 shows dimensionless deflections for the primary ($\bar{v}_1$) and secondary ($\bar{v}_2$) beams for a speed factor $\alpha = 1$ and different values of damping ratio ζ and stiffness parameter β. The figure shows that, in general, the system behaves as in the case for a speed factor $\alpha = 0.5$. Also for very small (decoupled) and very high (rigid-coupled) values of the stiffness parameter β, the absolute maximum value of $\bar{v}_1$ is reached after the load departs from the beam. For the case of elastic coupling, this value is reached short before the load left the beam. That is because a variation of the stiffness parameter leads to a variation of the circular natural frequency Ω_n, given in Eq. (33). Figs. 5a$_2$–e$_2$ show that the absolute maximum value of $\bar{v}_2$ is reached after the load departs from the beam.

Fig. 6 shows the normalized maximum deflections of the primary beam $\bar{v}_{1,\max} = v_{1,\max}/v_0$ and the secondary beam $\bar{v}_{2,\max} = v_{2,\max}/v_0$ versus the speed parameter α for different values of stiffness parameter β and damping ratio ζ calculated at $x = L/2$. From the Figure the following characteristics can be noted:

1. The maximum deflections $\bar{v}_{1,\max}$ and $\bar{v}_{2,\max}$ of a double-beam are smaller than $\bar{v}_{\max}$of a single beam as presented by Fryba [10] and Pesterev [11].
2. For small values of stiffness parameter β, an increase in the damping leads to a decrease in $\bar{v}_{1,\max}$ of the primary beam and an increase in $\bar{v}_{2,\max}$ of the secondary beam. However, for higher values of β, the system behaves reversely.
3. Increasing the values of the stiffness parameter β leads to a decrease in $\bar{v}_{1,\max}$ and an increase in $\bar{v}_{2,\max}$ at the same time.
4. For very high values of β, the maximum deflections $\bar{v}_{1,\max}$ and $\bar{v}_{2,\max}$ coincide with each other and take values equal to $0.5\bar{v}_{\max}$ of a single beam.

Fig. 7 shows the normalized force transmitted $\bar{F}_T = F_T/P_0$ between the primary and secondary beams calculated at $x = L/2$ versus the dimensionless time s for different values of speed factor α, damping ratio ζ, and stiffness parameter β. From the figure the following can be noted:

1. Increasing the damping leads to an increase in $F_{T,\max}$ by relative small values of stiffness parameter β (Fig 7a–c) and to a decrease in $F_{T,\max}$ by higher values of β (Fig. 7d–f).
2. By increasing the damping, the maximum value of the force transmitted $F_{T,\max}$ occurs at an earlier time.
3. The effect of damping is high by small values of stiffness parameter and low by higher values of this parameter.
4. In general, increasing the speed parameter leads to an increase in the maximum value of the force transmitted.

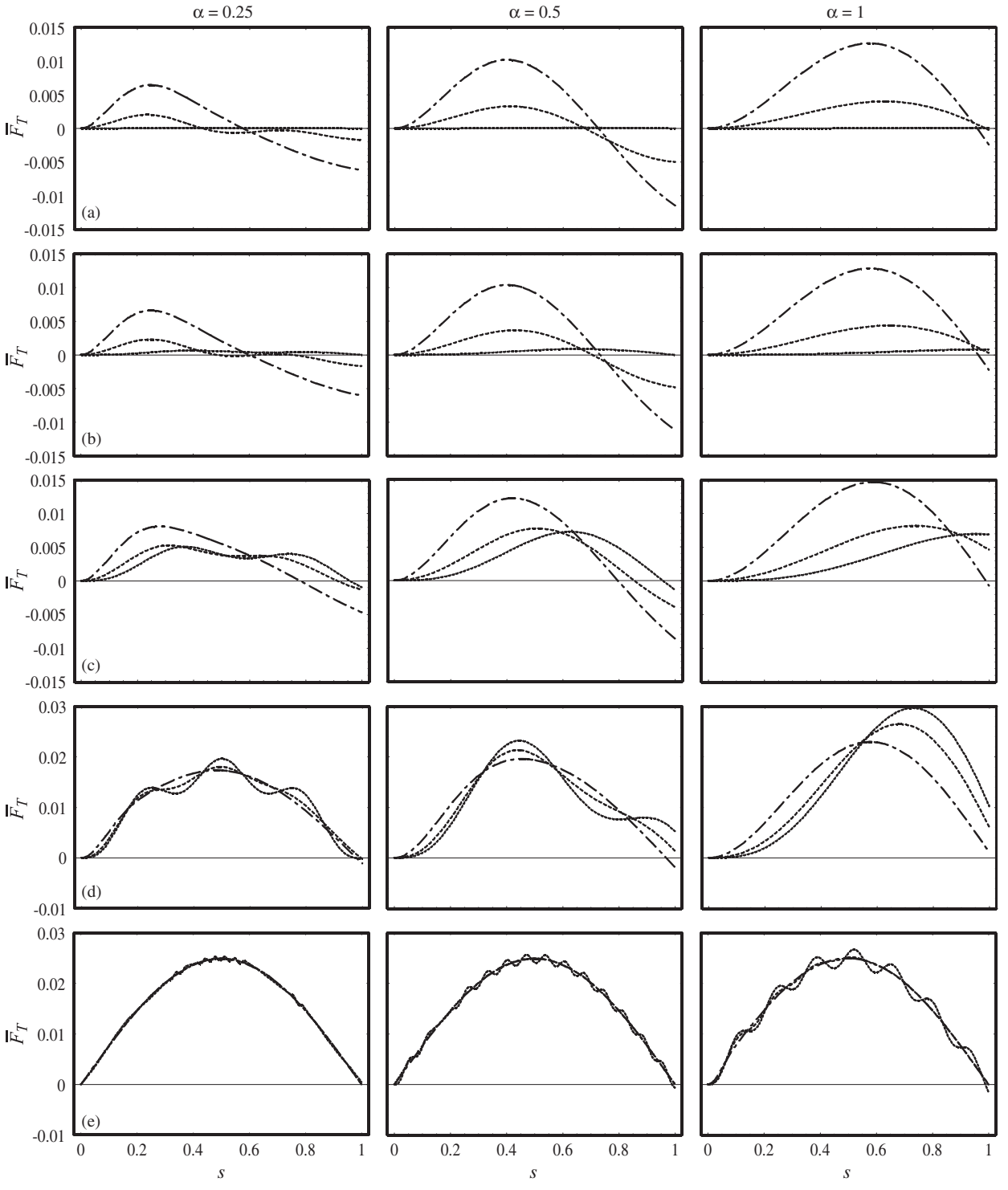

Fig. 7. Normalized force transmitted $\bar{F}_{T,\max}$ between the beams versus the dimensionless time s for different values of speed factor α, stiffness parameter β, and damping ratio ζ calculated at $x = L/2$: (———) $\zeta = 0$, (……) $\zeta = 0.1$, (— · — · —) $\zeta = 0.5$. (a) $\beta = 0.1$, (b) $\beta = 1$, (c) $\beta = 10$, (d) $\beta = 100$, (e) $\beta = 10\,000$.

4. Conclusions

The dynamic response for a simply supported homogeneous isotropic double-beam system subject to a moving constant load was investigated. The normalized deflections of both beams are obtained in closed forms. Also several plots of the deflections of the beams are given and discussed. The effects of the moving speed of the load and the damping and stiffness of the viscoelastic layer on the deflections of the beams are explored. It is found that increasing the damping of the connecting viscoelastic layer may increases or decreases the responses of the beams. However, this damping has negligible effect on the deflections of the beams for very high values of the stiffness of the layer. Furthermore, it is found that increasing the stiffness of the layer decreases the deflection of the beam on which the load travels (primary beam) and increases the deflection of the secondary beam. In case of very high layer stiffness, both beams have the same deflection since the beams are then rigid-coupled and behave as a unit. This deflection is half the dynamic deflection of a single beam traversed by a constant load moving with a constant speed.

References

[1] Z. Oniszczuk, Free transverse vibrations of elastically connected simply supported double-beams complex system, *Journal of Sound and Vibration* (232) (2000) 387–403.
[2] H.V. Vu, A.M. Ordonez, B.H. Karnopp, Vibration of a double-beam system, *Journal of Sound and Vibration* (229) (2000) 807–822.
[3] Z. Oniszczuk, Forced transverse vibrations of an elastically connected complex simply supported double-beam system, *Journal of Sound and Vibration* (264) (2003) 273–286.
[4] M. Shamalta, A.V. Metrikine, Analytical study of the dynamic response of an embedded railway track to a moving load, *Archive of Applied Mechanics* (73) (2003) 131–146.
[5] T.R. Hamada, H. Nakayama, K. Hayashi, Free and Forced vibration of elastically connected double-beam systems, *Bulletin of the Japan Society of Mechanical Engineers* (1983) 1936–1942.
[6] M. Gürgöze, H. Erol, On laterally vibrating beams carrying tip masses, coupled by several double spring–mass systems, *Journal of Sound and Vibration* (269) (2004) 431–438.
[7] Z. Oniszczuk, Transverse vibrations of elastically connected double-string complex system—part I: free vibrations, *Journal of Sound and Vibration* (232) (2000) 355–366.
[8] Z. Oniszczuk, Transverse vibrations of elastically connected double-string complex system—part II: forced vibrations, *Journal of Sound and Vibration* (232) (2000) 367–386.
[9] H. Erol, M. Gürgöze, Longitudenal vibrations of a double-rod system coupled by springs and dampers, *Journal of Sound and Vibration* (276) (2004) 419–430.
[10] L. Frýba, *Vibration of Solids and Structures Under Moving Loads*, Noordhoff International, Groningen, 1972.
[11] A.V. Pesterev, B. Yang, L.A. Bergman, C.A. Tan, Revisiting the moving force problem, *Journal of Sound and Vibration* (261) (2003) 75–91.